Towards a better understanding and prediction of the bremsstrahlung background in PIXE spectra

David D. Cohen, Ed Stelcer, Michael Prior, Rainer Siegele and Mihail Ionescu
ANSTO, PMB1, Menai, NSW, 2234, Australia.

Abstract

Murozono and Ishii et al recently published theoretical QFEB, SEB and AB bremsstrahlung cross sections which, when modified by typical X-ray detection efficiencies, provide excellent predictions of the backgrounds in PIXE spectra for a range of light target matrices.

Introduction

MeV ions impinging on solid targets produce bremsstrahlung radiation. For MeV ions on light to medium atomic numbered targets this radiation has at least three components; quasifree electron (QFEB), secondary electron (SEB) and atomic bremsstrahlung (AB)[1-4]. The QFEB process is represented schematically in Fig. 1. A target electron is scattered by the Coulomb field of the projectile producing bremsstrahlung x-rays. The cross section becomes large when the projectile velocity

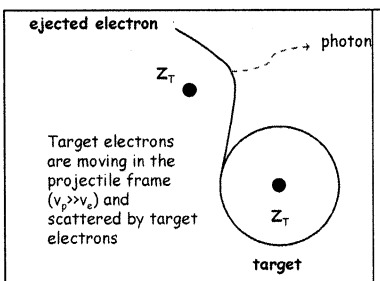

Fig. 1. Schematic QFEB

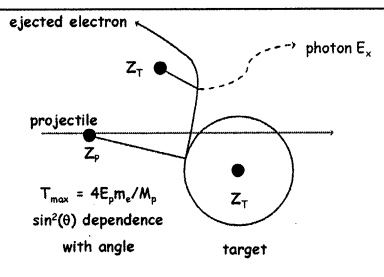

Fig. 2. Schematic SEB.

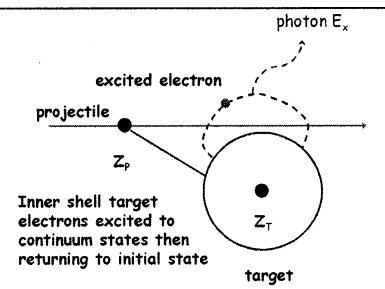

Fig. 3. Schematic AB.

is much larger than the target electron velocity. The maximum energy transferred to the electron at rest is $[T_r=m_eE_p/M_p]$. The SEB radiation is produced when the projectile ejects a target electron which is then scattered by the Coulomb field of another target nucleus. This process is shown in Fig. 2.

The maximum energy transferred to the target electron in this SEB process is $[T_m= 4T_r= 4m_eE_p/M_p]$. The final bremsstrahlung process we consider here is AB shown in Fig. 3. This occurs when a bound target electron is excited to the continuum, by the projectile and then returns to its original bound state. This results in a continuous spectrum from a few eV to tens of keV depending on the bound state of the electron. Following Murozono et al [4] we only consider K and L shell bound states here. Typical cross sections for 3MeV protons on carbon for these three

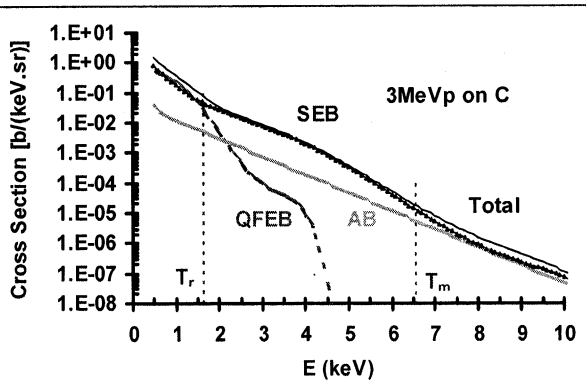

Fig. 4. Typical cross sections for QFEB, SEB and AB processes for 3 MeV protons on carbon after Murozono et al [4].

mechanisms are shown in Fig. 4. The QFEB process is significant below 2keV, SEB dominates the total bremsstrahlung cross sections from 2-8keV and AB becomes significant above 8keV x-ray energies. For 3MeV protons on carbon T_r=1.6 keV and

T_m=6.5keV which is reflected well in the cross section fall off in the QFEB and SEB data of Fig. 4 (see vertical dashed lines). These bremsstrahlung cross sections are monotonic and continuous with X-ray energy and increase significantly with decreasing energies below 10 keV.

Particle Induced X-ray Emission (PIXE) experiments [5,6] are generally performed using 3MeV protons on carbon like matrices with silicon based detection systems. Fig. 5 shows the calculated detection efficiency for a typical Si(Li) detector with 25μm beryllium entrance window thickness and two different crystal dead layer thicknesses of 0.1μm and 0.5μm [7]. Discontinuities are produced in the detection efficiency at the Si K edges and the gold contact M edges as shown [8].

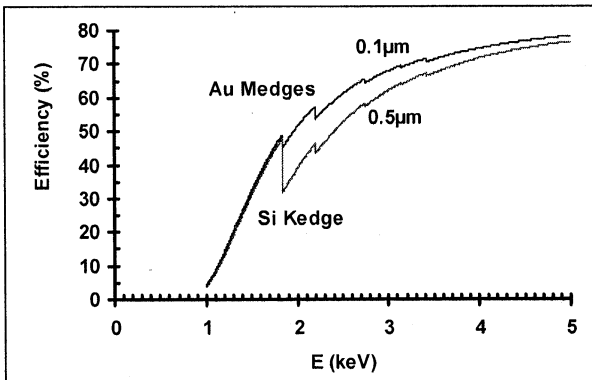

Fig. 5. Typical efficiency for a Si(Li) detector with 25 μm thick beryllium entrance window and dead layer thicknesses of 0.1 and 0.5 μm, after Cohen [7].

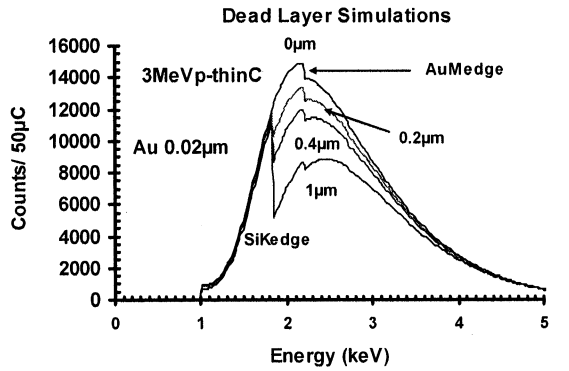

Fig. 6. Bremsstrahlung yield simulations for different dead layer thicknesses for 3 MeV protons on 2.7 mgcm^{-2} thin carbon.

The drop in efficiency from 100% above 10 keV to less than 1% at 1 keV folds the cross section plots of Fig. 4 over below 2 keV, producing the classic measured PIXE bremsstrahlung shapes shown in the simulations of Fig. 6 for 3 MeV protons on thin carbon. The discontinuities at the Si Kedge and the gold contact layer M edges have been used by Cohen et al [8] to estimate the detector silicon dead layer and the gold contact layer thicknesses.

Bremsstrahlung Yields

Scaling the QFEB, SEB and AB cross sections of Murozono et al [4] and convoluting their sum over the 0-15keV X-ray energy region with the detection efficiencies of Cohen [7] we can calculate the total bremsstrahlung yields for different ions on selected targets. Fig. 7.

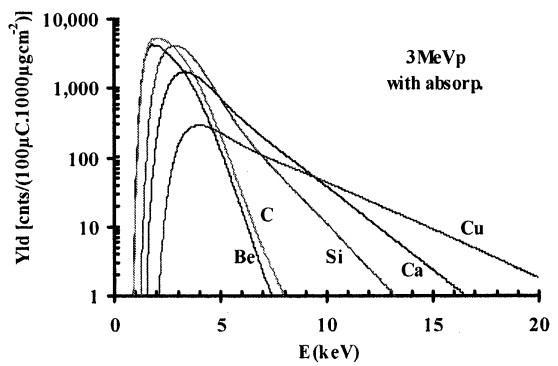

Fig. 7. Calculated bremsstrahlung yields for 100 μC of 3 MeV protons, using a detector with 80 μm Be window and solid angle of 1.3msr. All targets were 1,000 μgcm^{-2} thick.

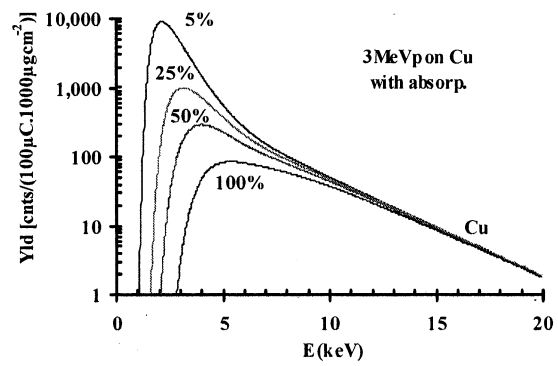

Fig. 8. The variation in bremsstrahlung yields with target self absorption, using 5%, 25%, 50% and 100% of the target thickness for self absorption corrections on a Cu target.

shows such a calculation for 100μC of 3 MeV protons on 1,000 μgcm^{-2} Be, C, Si, Ca and Cu targets. Note the target thickness is much less than the proton range. These yields have been corrected for detection efficiency and self absorption of 3 MeV protons for all targets. As the target atomic number Z_2 increases the X-ray yields increase in the 7-20 keV region. The peak in the bremsstrahlung shifting from 2 keV for Be to 4 keV for Cu targets is produced by self absorption in the target. This is clearly demonstrated by Fig. 8 where yields for 3 MeV protons on 1,000 μgcm^{-2} thick Cu are plotted as a function of the percentage depth at which the self absorption was calculated. Self absorption shifts the low energy cut off and the apparent peak in the yield to higher X-ray energies as the size of the correction increases with depth.

We have measured bremsstrahlung yields from a range of pure thin targets including Be and C. Fig. 9 shows such yields for 200 μC of 2, 3 and 4 MeV protons on 1,767 μgcm-2 thick carbon. For proton energies above 2.2 MeV on carbon an additional Compton scattered gamma ray background component appears in the spectrum above 10 keV. This can be adequately fitted by an exponential function in X-ray energy and subtracted off, leaving the pure bremsstrahlung component, between 0 and 10 keV, see Cohen et al [9].

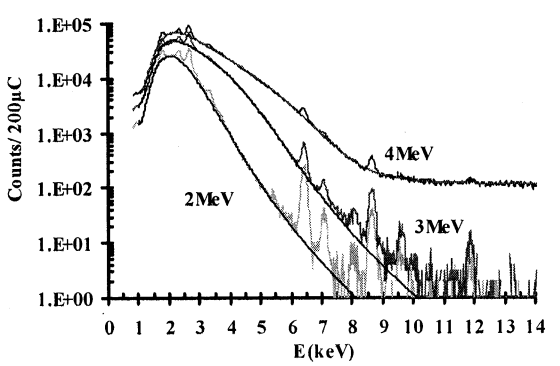

Fig. 9. Experimental yields for 2, 3 and 4 MeV protons on 1767 μgcm^{-2} thick carbon.

The solid curves of Fig. 9 show the background shapes of these PIXE spectra were well fitted by the bremsstrahlung plus gamma ray backgrounds calculated above. Indeed Figs 10 and 11 show that this technique for bremsstrahlung prediction can be used to fit thin targets for compounds as well as pure elements. Fig 10 is the PIXE spectrum for 2.6MeV protons on thin Teflon. The Teflon was relatively very pure and hence the spectrum well represents bremsstrahlung background. The flat continuous background above 10keV was due to Compton scattered gamma rays from F(p,p'γ) reactions and was well fitted by an exponential function in x-ray

energy all the way down to zero keV. The solid curve under the experiment between 1 and 9 keV was the predicted bremsstrahlung background for (CF_2) Teflon with only one extra parameter for scaling its peak height to fit the experiment between 2 keV and 3 keV. Closer inspection shows a good fit to the experimental shape, with significant deviation only above 4 keV where the AB component maybe underestimated by theory.

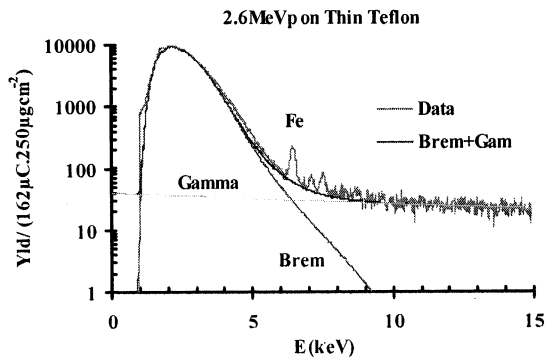

Fig. 10. Comparison of experimental and theoretical bremsstrahlung backgrounds for 2.6 MeV protons on 250 μgcm^{-2} Teflon $(CF_2)_n$ target.

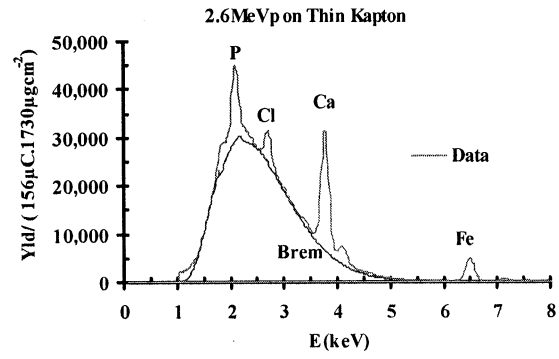

Fig. 11. Comparison of experimental and theoretical bremsstrahlung backgrounds for 2.6 MeV protons on 1730 μgcm^{-2} Kapton $(C_{22}H_{10}N_2O_5)_n$ target.

This may be expected since the AB contributions calculated by Murozono et al [4] only included the K and L shell target electrons and only transitions from these levels to the continuum and back to the K or L shell. Whereas one might expect transitions from inner shell target levels to the continuum (Radiative Ionisation, RI) may also contribute in this X-ray energy region [2]. The excess counts in this region may be due to pileup of the bremsstrahlung radiation with itself although experimental count rates were kept low so that dead time corrections were typically well below 5% for most runs.

Fig. 11 is a similar plot to Fig. 10 except for thin Kapton $(C_{22}H_{10}N_2O_5)_n$, this was plotted on a linear scale so the background fit below the characteristic peaks for P, Cl K and Fe could be better assessed. Again the fit was excellent with the only fitting parameter being a single scaling factor to match theory and experiment in the 3 keV region where there were no characteristic X-ray peaks.

Summary

Theoretical QFEB, SEB and AB cross sections have been used to estimate the experimental bremsstrahlung backgrounds found in typical thin target PIXE spectra of pure elements for proton energies between 1 and 4 MeV. This has been extended, again with good results, to compounds containing lighter elements like carbon, oxygen, nitrogen and fluorine. If the Compton scattered gamma ray background was simulated with an exponential function in X-ray energy, then the total background for most common PIXE spectra were successfully modelled from first principals. These concepts can now be included into standard PIXE analysis codes like PIXAN [10,11], GUPIX [12,13] and GeoPIXE [14].

Acknowledgements

We would like to acknowledge the help of the 2 MV STAR accelerator staff in several aspects of this work. This work was partly performed within the framework of IAEA CRP G.4.20.02 Unification of nuclear spectrometries.

References

[1] F. Folkmann, C. Gaarde, T. Huus, K. Kemp, Nucl. Instr. Meth., 116 (1974) 487-499.

[2] K. Ishii, S. Morita, Nucl. Instr. Meth., B22 (1987) 68-71.

[3] K. Ishii, Radiation Physics and Chemistry, 75 (2006)1135-1163.

[4] K. Murozono, K. Ishii, H. Yamazaki, S. Matsuyama, S. Iwasaki, Nucl. Instr. Meth., B150 (1999) 76-

[5] S. A. E. Johannson and J.L. Campbell, "PIXE: A Novel Technique for Elemental Analysis", Wiley and Sons, New York, 1988.

[6] D. D. Cohen and E. Clayton, "Ion Induced X-ray Emission" in "Ion Beams for Materials Analysis", eds.J. R. Bird and J.S. Williams (Academic Press, Sydney, 1989) Chap 5.

[7] D. D. Cohen, Nucl. Instr. Meth., 178 (1980) 481-490.

[8] D. D. Cohen et al, submitted to X-ray Spectrometry 2007.

[9] D. D. Cohen et al, submitted to Nuclear Instr. Meth., 2007.

[10] E. Clayton, D. D. Cohen and P. Duerden, Nucl. Instr. Meth., B22 (1987) 64.

[11] D. D. Cohen and E. Clayton, Nucl. Instr. Meth., B22(1987)59.

[12] J. A. Maxwell, J. L. Campbell, W.J. Teesdale, Nucle Instr. Meth. B43 (1989) 218.

[13] J. A. Maxwell, W.J. Teesdale, J. L. Campbell, Nucle Instr. Meth. B95 (1995) 407.

[14] C. G. Ryan, D. R. Cousens, S. H. Sie, W. L. Griffin, Nucl. Instr. Meth. B49 (1990) 217.